

Avinash Gudimetla^{1*}, D Lingaraju², S Sambhu Prasad³

¹Research Scholar, Department of Mechanical Engineering, JNTUK, Kakinada, Andhra Pradesh, India

²Department of Mechanical Engineering, University College of Engineering, JNTUK, Kakinada, Andhra Pradesh, India

^{1,3}Department of Mechanical Engineering, Pragati Engineering College, Surampalem, Andhra Pradesh, India

*Corresponding author. E-mail: avinashdattu1@gmail.com

Received (Otrzymano) 4.11.2020

INVESTIGATION OF MECHANICAL AND TRIBOLOGICAL BEHAVIOR OF Al 4032-SiHGM MMC

The present study is aimed at identifying the influence of silicon hollow glass microspheres (SiHGM) on a newly engineered metal matrix composite. Silicon micro balloons of various wt.% (2, 4, 6) are reinforced in to aluminium 4032 to produce a composite using the stir casting technique. The mechanical properties of the composite such as hardness, tensile and compressive strength were measured. The dry sliding wear test was conducted on the produced specimens to measure the wear rate and coefficient of friction. The results revealed that the properties of the composite are better with an increase in the wt. % of reinforcement. The presence of reinforcement in the composites was identified using Energy Dispersive X-Ray analysis (EDX). The grain boundaries and grain refinement for various compositions of reinforcements and worn surfaces were analyzed using Scanning Electron Microscope (SEM) micrographs. The process parameters for the minimum wear rate and coefficient of friction were identified and optimized by using the Taguchi L₁₆ orthogonal array. Analysis of variance (ANOVA) was used to determine the percentage contribution of each process parameter. Multi-response optimization was carried out using Grey relational analysis (GRA) to optimize the process parameters to attain a minimum coefficient of friction and wear rate. The variation in wear rate and coefficient of friction are analyzed with respect to reinforcement (wt.%), speed (rpm) and load (N).

Keywords: silicon hollow glass microspheres, stir casting, pin on disc, wear rate

INTRODUCTION

Important mechanical properties such as light weight, high specific strength and specific stiffness can be obtained by metal matrix composites, which cannot be achieved by any of the individual components. They exhibit good dimensional stability, resistance to temperature, wear and good inclination to casting. Because of these properties, metal matrix composites, particularly aluminium metal matrix composites find applications in a wide range of fields such as aerospace, automotive, defense, mining, sports and electronic industries as well as in recreation [1, 2]. The wide usage of these composites is limited because of the difficulty in their fabrication. The stir casting technique is a less expensive method for the fabrication of composites. It is widely used because of its capability in producing composites with a better matrix-reinforcement interface, which helps to achieve better mechanical and tribological properties [3]. The research on silicon microballoons as reinforcement in metal matrix composites is modal; hence in this study, an attempt is made to understand the behavior of Al4032, when it is reinforced with various wt.% (2, 4, 6) of silicon hollow glass microspheres. The composites were prepared using the stir casting technique by incorporating rein-

forcement of the required proportions into the matrix material. Specimens were made from the produced composites, according to ASTM standards for testing. Energy Dispersive X-Ray Analysis (EDX) was performed on the prepared specimens to obtain the information relating to the existence of reinforcements in them. The hardness, micro-hardness, tensile and compressive strength values of the composites were measured by subjecting the specimens to tests. The variation in the grain structure of the composites from the base metal and bonding of the reinforcement to the matrix was analyzed using micrographs obtained by means of a Scanning Electron Microscope (SEM). Furthermore, these micrographs were used to ascertain the average grain size of the composites, which helps to understand the variation in properties of the composite with respect to the change in grain size.

The wear pattern of the specimens at room temperature was studied from micrographs obtained by SEM. The prepared composites show a boost in the mechanical properties with a decrease in the wear rate and coefficient of friction when compared to the base material. Reinforcement (wt.%), speed (rpm) and load (N) are the process parameters considered in this investigation.

Taguchi L_{16} orthogonal array was considered to obtain the optimal process parameters for the minimum wear rate. Also, by using the same orthogonal array, optimized process parameters to obtain the minimum coefficient of friction were found. Analysis of variance (ANOVA) was conducted individually on the responses i.e., the wear rate and coefficient of friction to obtain the contribution of the process parameters. Multi response optimization to obtain the minimum wear rate and minimum coefficient of friction were found by performing Grey Relational Analysis (GRA).

EXPERIMENTAL PROCEDURE

Material selection

Al4032 is the matrix material that was chosen for this study whose chemical composition is shown in Table 1. Silicon hollow glass microspheres with high performance and of a 50 μm size were chosen as the reinforcement whose SEM micrograph is shown in Figure 1 and the details of the reinforcements are shown in Table 2. Reinforcement with various compositions of wt.% (2, 4, 6) were introduced into the matrix material to produce the required composites.

TABLE 1. Composition of Al 4032

Element	Al	Si	Cu	Mg	Ni	Fe
wt. %	83.78	13.2	1.0	1.1	0.9	0.02

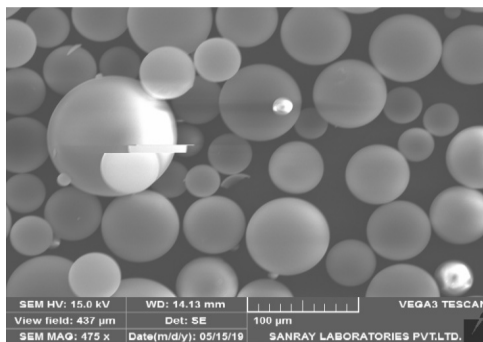


Fig. 1. SEM micrograph of silicon microballoons

TABLE 2. Details of reinforcement

Reinforcement	Grain size [μm]	Density [g/cm^3]	[wt.%]
SiHGM	50	0.27	2, 4, 6

Composite fabrication

In this work, the composite was synthesized by the stir casting technique. The matrix material procured in the form of a bar was machined in to small pieces. An electrical muffle furnace, placed vertically was used to melt the matrix material. The furnace was maintained at the temperature of 900°C , which is above the melting

temperature of the matrix material, and was preheated at that temperature for 30 minutes. The matrix material in the required composition was weighed and then put into a graphite crucible, which was placed in the furnace. The reinforcement was preheated simultaneously in a heater for a period of $15\div 30$ minutes at 250°C to remove the presence of moisture present (if any) in them. After the matrix material in the crucible reached its molten form, it was maintained at the temperature for few minutes. The required amounts of reinforcement material in different proportions were added to the molten material. A mechanical stirrer was prepared to suit the furnace and was placed in the crucible from the top and was maintained to run at $200\div 300$ rpm with the help of a motor and regulator for about $3\div 5$ minutes. The stirrer was adjusted to such a height that spilling of the molten metal from the crucible was avoided. The height of the stirrer can be adjusted based on the volume of metal that was present in the crucible. The stirrer was provided with a plate, which has a provision for the shaft of the stirrer and a hole to introduce the reinforcement. The hole was closed after adding the reinforcement. This plate was placed on the top of the crucible to avoid interaction of the metal with the atmosphere. This plate also served an additional purpose of creating small vibrations, which help to better distribute the reinforcement in the matrix. 1 wt.% of magnesium was added to increase the wettability between the matrix and reinforcement and the chances of agglomerating was reduced. Degassing tablets were used during the melting process to remove the gases that were produced therein. Also 1 wt.% of ammonium chloride was added to the melt, which acts as a coverall flux and prevents oxidation from atmospheric air. Finally, the molten metal was poured in to a cast iron mold, pre-heated to the temperature of 450°C . After the molten metal was poured into the mold, it was covered with husk so as to maintain the temperature for directional solidification, which also enhanced the mechanical properties.

Density and porosity measurement

The theoretical density of the composites was found by the rule of mixtures. The experimental densities of the composites were calculated by the Archimedes principle, by weighing the sample in air and in water. The density measurements were made as per ASTM D 792 standards. The effect of porosity during casting cannot be fully avoided and can be minimized by taking proper precautions.

Hardness test

Hardness tests were conducted on the matrix material and the produced castings as per ASTM E18 standards. From each composite produced with various wt.% (2, 4, 6) of reinforcement, one sample was selected for testing. The surface of the selected samples

was grinded with emery papers and further polished on a polishing machine to make the surfaces highly polished. A load of 100 kg was applied for a dwell time of 20 s with a 1/16" ball indenter. Three random locations were selected by maintaining minimum a distance between the locations and the test was conducted to obtain the average value of hardness.

Vickers micro hardness test

The specimens were prepared for as the hardness test, then, selected and highly polished for testing in a Vickers micro hardness testing machine. This test is intended for finding the surface hardness of the specimens. From each composite produced with various wt.% (2, 4, 6) of reinforcement, one sample was selected for testing and the test was performed as per ASTM E10-07 standards. Each specimen was loaded with 200 g, which was applied for a dwell time of 15 s. Five random locations were selected, maintaining a minimum distance between the locations, and the test was conducted to obtain the average value of hardness.

Tensile test

Tensile tests were conducted on a universal testing machine at room temperature on machined specimens and the values for the yield strength, ultimate tensile strength and % of elongation were found. From each composite produced with various wt.% (2, 4, 6) of reinforcement, one sample was selected for testing and the test was performed according to ASTM E8 standards.

Compression test

The compression test was conducted on a compression testing machine at room temperature on all the machined specimens to study the behavior of the composites under compressive load [4]. From each composite produced with various wt.% (2, 4, 6) of reinforcement, one sample was selected for testing and the test was performed as per ASTM E09 standards. Medium-sized samples with a diameter of 13 mm, length 39 mm and L/D ratio 3 were used to assess the compression strength. The values of ultimate compressive strength were obtained from the compression test.

Microstructure study

Micro-structural characterization of the composites was performed on micrographs produced by SEM. One sample from each composite produced with various wt.% (2, 4, 6) of reinforcement was selected for testing. The surface of the selected samples was grinded with emery papers of grit sizes 200, 300 and 400. They were further polished on a polishing machine to make the surfaces highly polished. These polished specimens were then cut according to the dimensions to fit under the SEM. These polished specimens were further etched

with a chemical agent known as Kellers reagent containing 190 ml distilled water, 5 ml nitric acid, 3 ml hydrochloric acid, and 2 ml hydrofluoric acid [5]. The specimens were subjected to the etchant for 15 s and were cleaned with distilled water. These specimens were then dried with hot air from a blower for 10 s. This process ensures better visibility of the microstructures. The micrographs were used to measure and analyze the grain structure as per the ASTE 112-96 procedure.

Wear and friction test

Wear and friction tests were performed on a pin-on-disc tribometer. The wear test was conducted on the specimens to study the tribological behavior of the composites under various process parameters. The test was performed under dry conditions at room temperature. The specimens were made from the cast composites as per G99 standards. A length of 25 mm with a cross-sectional area of 5 mmx5 mm was chosen as the dimensions for the pins to perform the test. For all the specimens, the surfaces to be tested were grinded with emery papers of grit sizes 200, 300 and 400. They were further polished on a polishing machine to make the surfaces highly polished and having a mirror finish, so that the machining irregularities on the surface do not affect the results of the test. The disc used in the wear test was made from EN32 steel. The specimens with the polished surface facing the disc were fixed and clamped to the lever with the aid of a screw setup. A sliding distance of 1.5 inches was adjusted with the lever. The amount of thickness lost from the specimen over a period of 3600 s was obtained from the test, which was used to estimate the wear rate. In addition, coefficient of friction was calculated from the obtained frictional force, by dividing it by the normal force.

OPTIMIZATION TECHNIQUE

Taguchi method

In order to reduce the cost and time associated with performing the experiment [6], the Taguchi technique is a proficient method for improving the performance of the experiment by optimal setting of the process parameters. The objective function, suggested by Taguchi for analysis of the results is the Signal to Noise ratio (S/N). The particular process parameters that affect the response and the contribution of these process parameters to the response can be obtained by performing ANOVA, which uses S/N as the prominent characteristic. The larger the better, the nominal the better and the smaller the better are the three categories of objective functions defined by Taguchi [6]. The chosen control factors, which affect the wear rate and coefficient of friction, are the reinforcement (wt.%), speed (rpm) and load (N). The various control factors and their levels are shown in Table 9. The Taguchi smaller the better

method is used in this analysis. The process parameters for the minimum wear rate and coefficient of friction are identified and optimized using the Taguchi L_{16} orthogonal array, and its layout is presented in Table 10. The analysis is carried out individually for both the wear rate and coefficient of friction.

ANOVA method

ANOVA is a traditionally used to ascertain whether the parameters in the experimental design have a prominent effect on the response or not. It also gives the quantitative value of each control factor on the response [7]. To identify the extent the factors affect the response, an F-test is conducted. The factors are considered as significant, if the value of P (probability $> F$) is less than 0.05, for a confidence limit of 95% [8]. In addition to that a large F value implies that the control factor has a substantial effect on the response. R^2_{adj} , the coefficient of adjusted correlation, is used to decide the extent of the fitted model. In order to ensure that the created model fits the well performed experiments, the values of R^2_{adj} and R^2 have to be high and close to one another. ANOVA was performed individually to determine the contribution of the control factors for minimum values of the wear rate and coefficient of friction for the composites.

RESULTS AND DISCUSSION

Density and porosity

The theoretical and measured densities, along with variation in the porosity of the matrix material and the composites are shown in Table 3. The density of the composite decreased with the increase in wt.% of reinforcement and this can be attributed to the presence of low density reinforcement, which reduced the density of the composites from 2.67 to 1.7 g/cm³ with SiHGM varying from 0 to 6 wt.%. Some portion of air or gas during casting becomes entrapped, resulting in porosity. The chance of the entrapment of gases is high during the casting process and the amount of porosity in the produced composites varies depending upon the constituents of the reinforcement and the method of fabrication. The amount of porosity can be calculated from the values of the theoretical and experimental densities. Porosity has an influential affect on the mechanical properties of the materials. Nonetheless, the presence of voids cannot be completely eliminated during the casting process. Therefore care should be taken to reduce the amount of porosity during casting. However, it can be minimized by adding degassing tablets to the molten metal before pouring into the mold. Even after due care, the addition of SiHGM also led to porosity in the produced composites and the amount of porosity rises with the increase in wt.% of SiHGM. This is because the interaction of the reinforcement with air grows as the wt.% of reinforcement increases, which

leads to a greater air envelope in the molten metal. The variation in density and porosity with respect to the reinforcement (wt.%) is shown in Figure 2.

Mechanical properties

The mechanical properties such as hardness, tensile strength and compressive strength were measured for Al 4032 with silicon microballoon reinforcement of various wt.% (2, 4, 6). The tests were conducted according to ASTM standards and at room temperature. The hardness, tensile strength and compressive strength values of the composites show an increase in their values with the increase in wt. % of the reinforcement. This is possible because of the uniform distribution of the reinforcements in the matrix material.

TABLE 3. Density of Al and Al MMC

Specimen No.	Matrix	Reinforcement	Reinforcement [wt.%]	Theoretical density [g/cm ³]	Experimental density [g/cm ³]	Porosity [%]
1	Al	Nil	0	2.68	2.67	0.37
2	Al	SiHGM	2	2.27	2.25	0.88
3	Al	SiHGM	4	1.97	1.94	1.52
4	Al	SiHGM	6	1.75	1.7	2.85

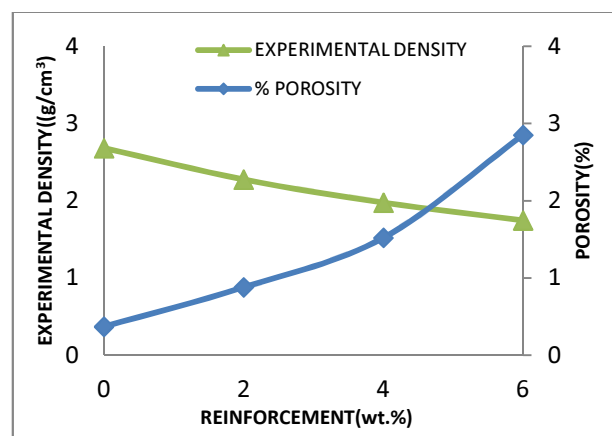


Fig. 2. Variation in density and porosity verses reinforcement (wt. %)

Hardness

The matrix material and the composites fabricated were subjected to hardness testing at room temperature [9]. The hardness values are shown in Table 4 and the variation in hardness with respect to reinforcement (wt.%) is shown in Figure 3a. It is observed that hardness value of the reinforced composites is higher when compared to the matrix material. The increase in hardness is because of the uniform distribution (Fig. 3b) of the reinforcement due to the combined effect of stirring and vibrations induced in the crucible during stirring.

TABLE 4. Hardness values of Al 4032 and Al MMC

Specimen No.	Matrix	Reinforcement	Reinforcement [wt.%]	HRB
1	Al	Nil	0	72
2	Al	SiHGM	2	80
3	Al	SiHGM	4	89
4	Al	SiHGM	6	94

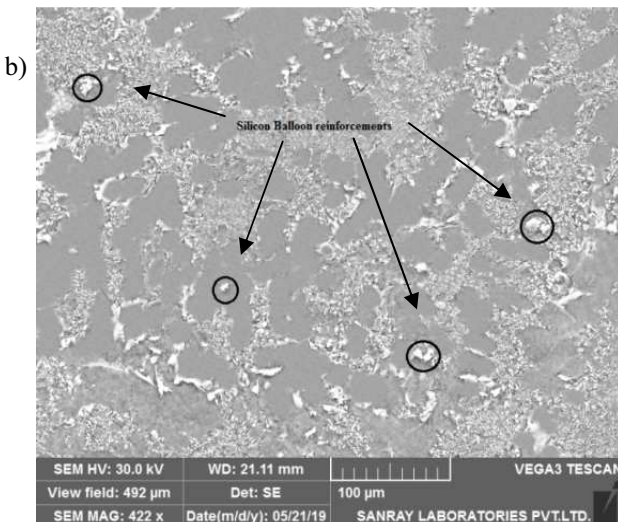
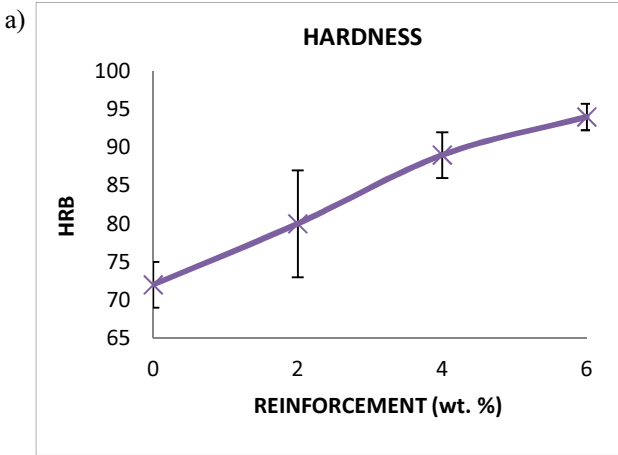


Fig. 3. Variation in hardness (HRB) with respect to reinforcement (wt.%) (a); distribution of silicon microballoons in Al4032 (b)

Micro hardness test

The surface hardness of the composites was obtained by conducting the Vickers microhardness test on the prepared specimens at room temperature. The results of the test revealed that the value of microhardness of the composites increased when compared to matrix material [10] and are shown in Table 5. The variation in the micro hardness values with respect to the reinforcement (wt.%) is shown in Figure 4. The micro hardness of the composites grew with an increase in reinforcement as the average spacing between the reinforcement decreases with an increase in reinforcement (wt.%). This rise in hardness of the composites can be attributed to grain refinement in the material because of the addition of reinforcement.

TABLE 5. Vickers hardness values of composites made by reinforcing Al 4032 with various wt.% of reinforcement

Specimen No.	Matrix	Reinforcement	Reinforcement [wt. %]	HV
1	Al	Nil	0	80.96
2	Al	SiHGM	2	107.02
3	Al	SiHGM	4	111.00
4	Al	SiHGM	6	118.10

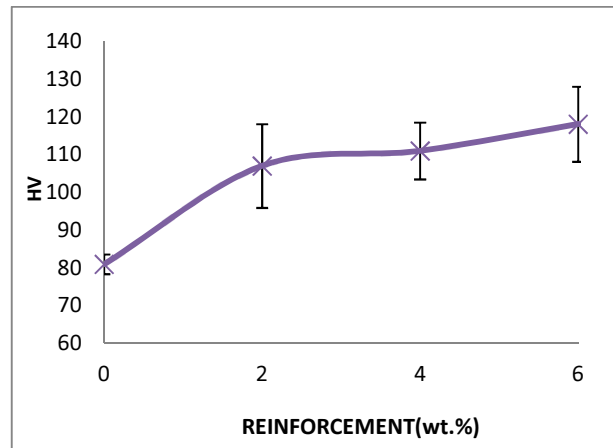


Fig. 4. Variation in Vickers microhardness (HV) with respect to reinforcement

Tensile strength

Various composites were prepared by adding silicon hollow glass microsphere reinforcement of various wt.% (2, 4, 6) to the Al 4032 matrix material. All these composites, along with base material were subjected to tensile tests on a universal testing machine following the standard procedure at room temperature [11]. The results obtained from the tensile tests are shown in Table 6 and the variation in yield strength, ultimate tensile strength and elongation with respect to reinforcement (wt.%) is shown in Figure 5. It is evident from the results that the yield strength and ultimate tensile strength of the produced composites are high when compared to the base metal and the values of yield strength and ultimate tensile strength rise with the increase in reinforcement (wt.%). The bonding between the reinforcement and matrix materials plays a key role in improving the yield strength and ultimate tensile strength of the developed composites. The presence of reinforcement in the matrix material acted as a nucleus and further grain refinement took place in the composites. What is more, the uniform size of the reinforcement particles and their spherical shape, along with their uniform distribution, contributed to the increase in the strength of the composites by transferring the load from low density regions in the matrix to high density regions near the reinforcement. This phenomenon raised the resistance of the material under tensile loading. Hence, the load required to cause failure increased.

TABLE 6. Tensile test results

Specimen No.	Matrix	Reinforcement	Reinforcement [wt.%]	Yield strength [MPa]	Ultimate tensile strength [MPa]	Elongation [%]
1	Al	Nil	0	309.25	363.32	10.4
2	Al	SiHGM	2	316.87	376.51	7.2
3	Al	SiHGM	4	323.49	390.98	4.8
4	Al	SiHGM	6	327.51	399.61	3.76

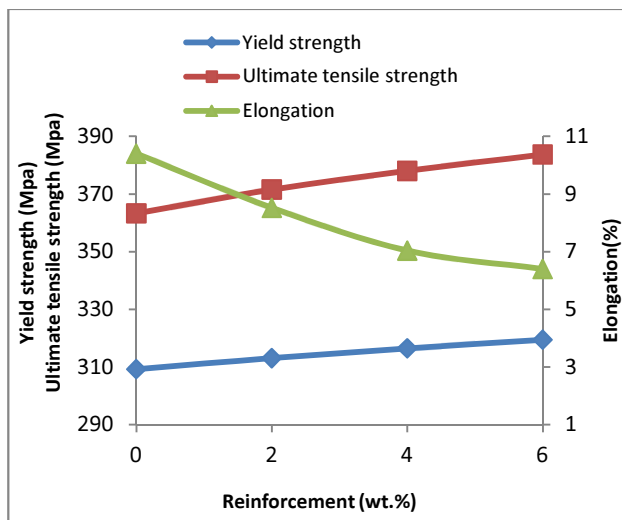


Fig. 5. Variation of yield strength, ultimate tensile strength and elongation with respect to reinforcement (wt.%)

Compressive strength

The compressive strength of the matrix material and composites with reinforcement of various wt.% (2, 4, 6) of silicon hollow glass microspheres was obtained by conducting the compression test at room temperature. The values of the ultimate compressive strength of the matrix material and the produced composites are shown in Table 7, and the variation in the ultimate compressive strength with respect to the reinforcement (wt.%) is shown in Figure 6. From the experimental values, it can be inferred that the ultimate compressive strength of the developed composites is high when compared to the matrix material. Furthermore, the values of strength rose with increase in wt.% of the reinforcement.

The presence of reinforcement created a nucleation and the grains are concentrated more around the nucleus. This grain growth created a change in the direction of crack propagation, to which the composites are capable of withstanding under a higher compressive load.

Moreover, the use of spherical hollow reinforcements raised the energy absorption ability of the composites. As a result of this, high stress levels are needed to propagate a crack to the dislocation densities to cause

failure, thereby increasing the compressive strength of the produced composites [12-14].

TABLE 7. Results of compression test

Specimen No.	Matrix	Reinforcement	Reinforcement [wt. %]	Ultimate compressive strength [MPa]
1	Al	Nil	0	411.2
2	Al	SiHGM	2	495.2
3	Al	SiHGM	4	568
4	Al	SiHGM	6	669.6

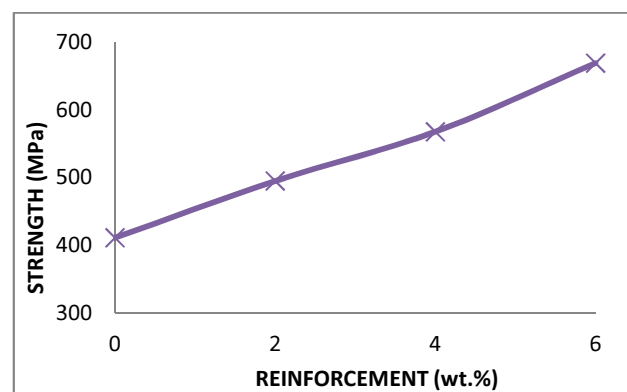


Fig. 6. Variation in ultimate compressive strength with respect to reinforcement (wt. %)

EDX analysis

EDX analysis was conducted to find the presence of reinforcing particles in the matrix material. Figure 7a-c shows the EDX analysis of the composites with 2, 4 and 6 wt.% of reinforcement. The high intensity peak of Si signifies the existence of reinforcement particles in the matrix material.

Micro-structural characterization

Scanning Electron Microscope (SEM) investigations were conducted on the samples prepared from Al 4032 reinforced with various wt. % of silicon microballoons. The surface of selected samples was grinded with emery papers of 200, 300 and 400 grit. These specimens were further polished on a polishing machine to make the surfaces highly finished and reflective. After polishing, the samples were etched with Kellers etch, a famous etchant for aluminum and its alloys. The specimens were etched for 25÷30 seconds. The specimens were then dried with a hot air gun to obtain better microstructure. Figure 8a-d shows the SEM micrographs of the matrix material and composites with silicon hollow glass microsphere reinforcement of various wt.% (2, 4, 6).

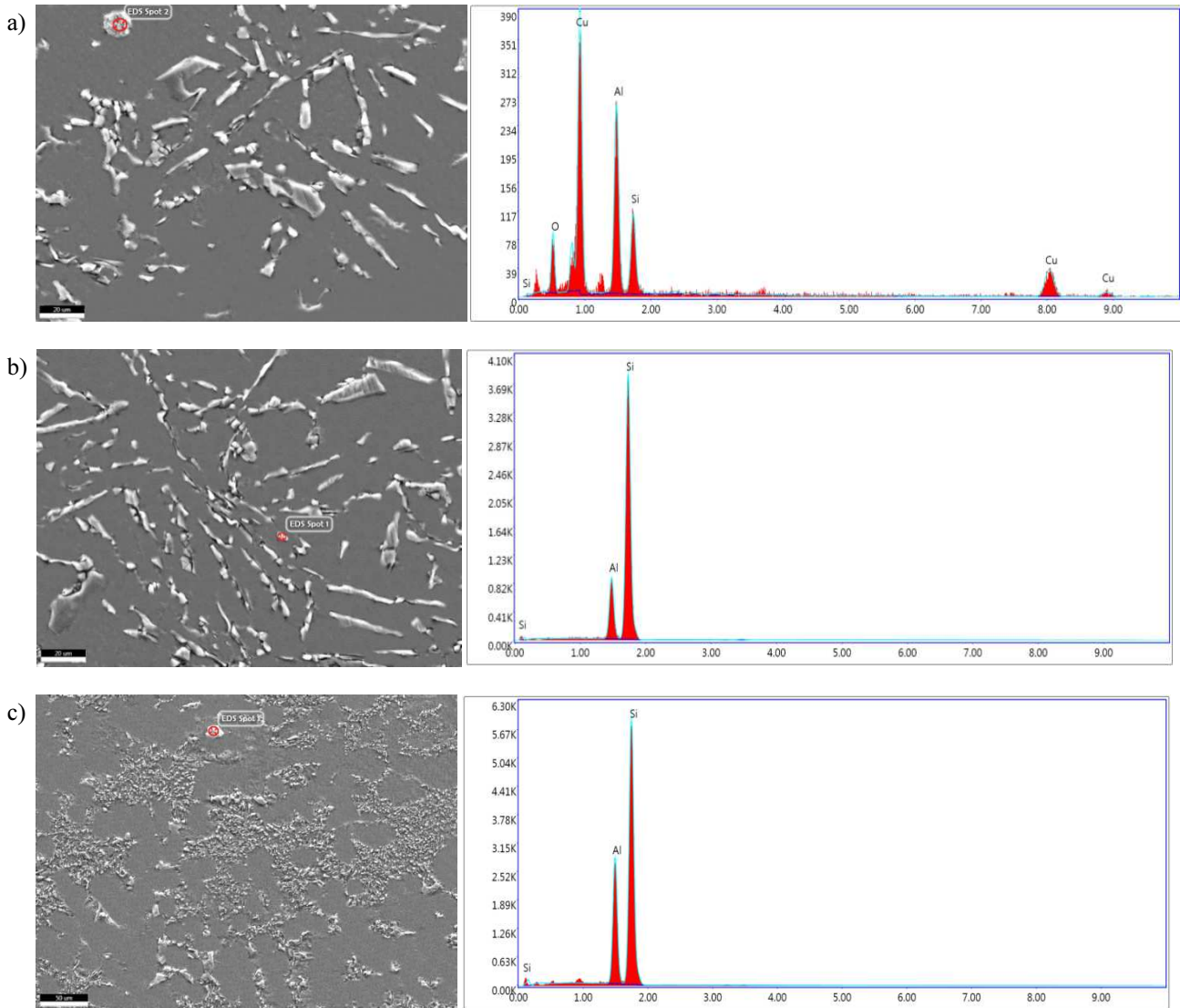


Fig. 7. a) EDX analysis of prepared composite with 2 wt.% reinforcement; b) EDX analysis of prepared composite with 4 wt.% reinforcement; c) EDX analysis of prepared composite with 6 wt.% reinforcement

The presence of secondary particles, a matrix phase, a matrix and alloy phase can be clearly observed in these micrographs. There is a change in morphology of the grains in the vicinity of the reinforcement [15]. The micrographs also reveal that there is good interfacial bonding between both the phases, with no crack formation. Figure 8a shows the microstructure of the matrix material with large dendrites and sparsely placed. Figure 8b-d shows there is a decrease in the length of the dendrites and rise in number of grains, with the increase in the wt.% of reinforcement. The grain size of the composites also falls with the increase in the wt. % of reinforcement, when compared to the matrix material [16] causing grain refinement. It can be observed from the SEM micrographs that the reinforcement is uniformly distributed. Furthermore, no agglomeration of the reinforcement was present at 2 and 4 wt.% of reinforcement with slight agglomeration at 6 wt.% of reinforcement. This phenomenon is due to the rejection of reinforcement from the matrix

material by the solidifying phase at the interface. The average grain size of the produced composites is measured from the SEM micrographs using ImageJ software and their values are shown in Table 8.

TABLE 8. Average grain size of composites prepared by reinforcing Al 4032 with various wt.% of reinforcement

Specimen No.	Matrix	Reinforcement	Reinforcement [wt.%]	Average grain size of matrix phase [μm]
1	Al	Nil	0	42.06
2	Al	SiHGM	2	30.88
3	Al	SiHGM	4	23.72
4	Al	SiHGM	6	15.21

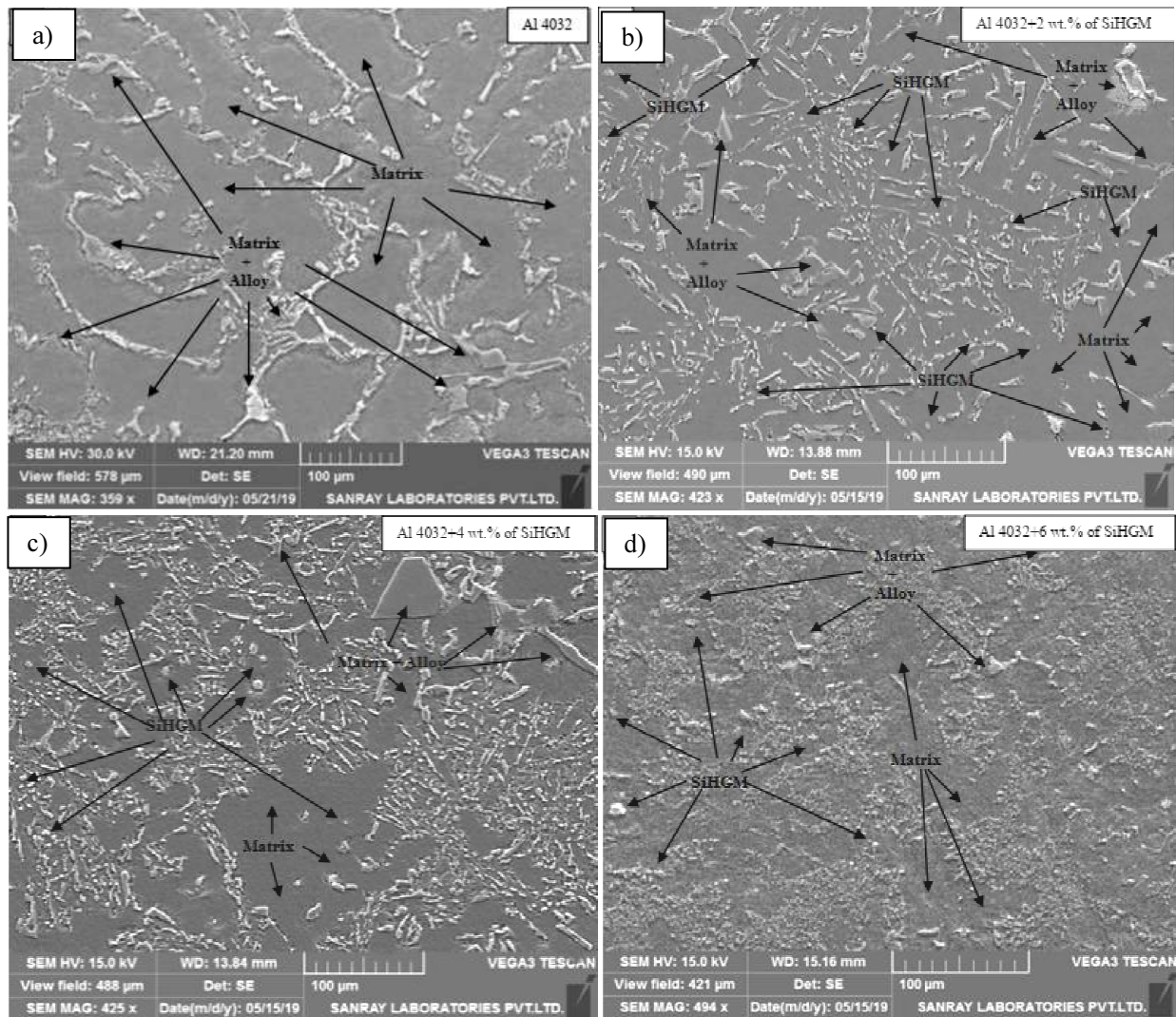


Fig. 8. SEM micrographs of matrix material and composites with silicon hollow glass microsphere reinforcement of various wt.% (2, 4, 6), showing matrix, matrix and alloy phases along with reinforcements (a-d)

Analysis of worn surface

Analysis of micrographs of the worn surfaces obtained from the SEM was performed to study the tribological characteristics of the Al 4032 composites in the absence of lubrication and at room temperature. Figure 9a-d shows the SEM micrographs of the matrix material and composites with silicon hollow glass microsphere reinforcement of various wt.% (2, 4, 6) at loads varying from 10 to 40 N, with intervals of 10 N and speeds varying from 100 to 700 rpm, with intervals of 200 rpm. It is observed from the microstructures that the formation of cracks [17, 18] takes place at higher speeds and loads, which leads to erosion of the surface because of de-lamination.

The presence of stronger reinforcement in the matrix phase obstructs the solidification of the matrix material. There is an increase in the number of grains and grain refinement, which is the result of the formation of nucleation sites in the matrix material by the reinforcing particles. This reduces the grain size of the matrix material.

As the material is subjected to higher speeds and loads, the material is subjected to high temperatures because of the rubbing from the rotating disc. The specimens with the increased wt. % of reinforcement are able to withstand these temperatures to a greater extent before being worn, as can be seen from the micro structures. The wear in the matrix material because of ploughing of the material in the form of chips is observed even at lower speeds and loads. Nevertheless, this phenomenon is observed in the produced composites at higher values of speeds and loads. The composites are deformed plastically because of high temperature, which cause a reduction in the strength of the reinforced composites and finally led to delamination and erosion causing wear [19, 20] of the material.

From the experiment results, it is observed that speed has predominant effect on the wear rate when compared to the effect of load, which was also revealed by the ANOVA results as shown in Table 15. The material exhibits a coarse structure and high wear in the form of worn out fibers, propagation of cracks and delamination at higher speeds.

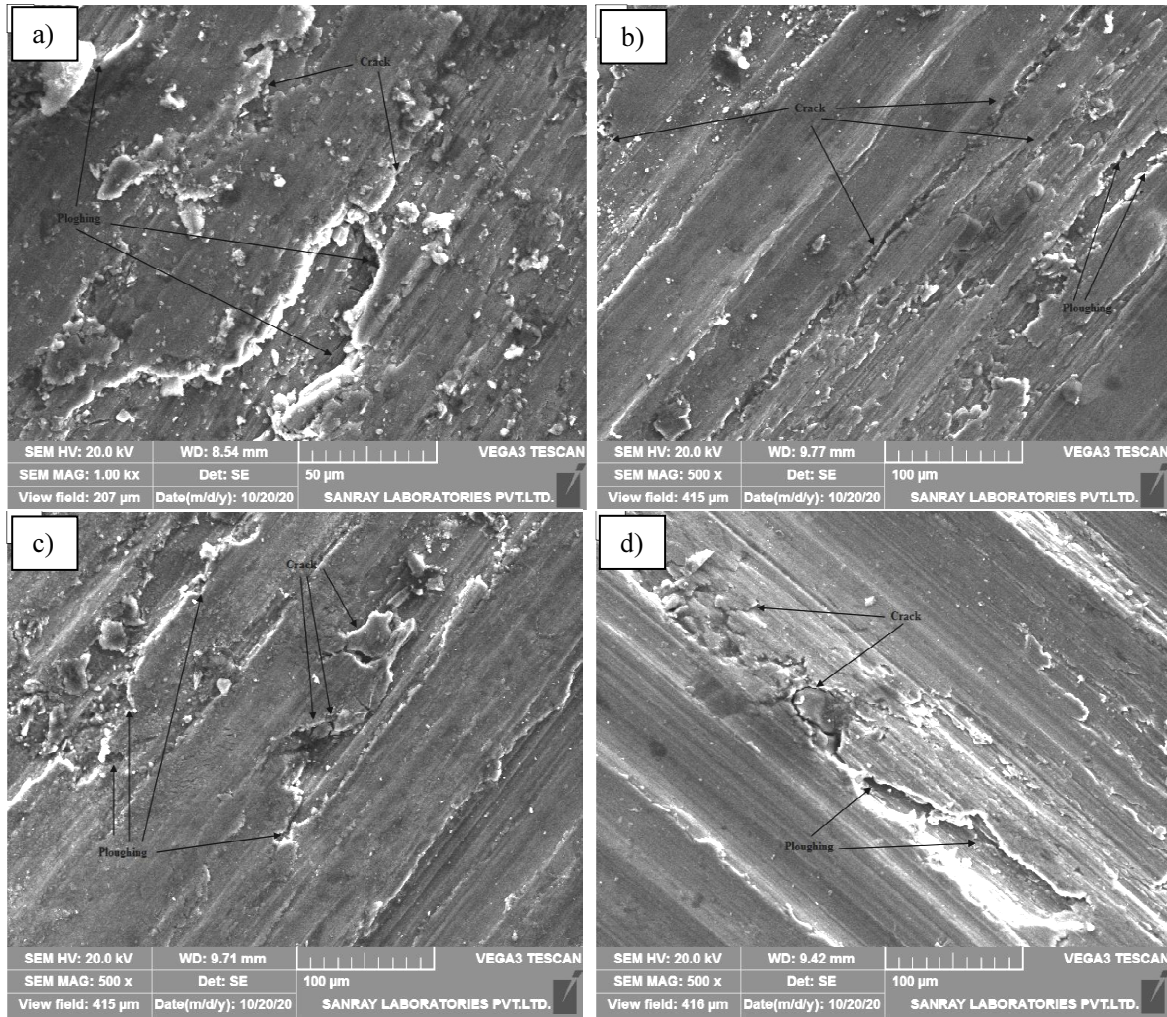


Fig. 9. SEM micrographs of surfaces after wear test of matrix material and composites with silicon microballoon reinforcement of various wt.% (2, 4, 6) at different loads and speeds (a-d)

Study of wear characteristics

Variation in wear rate with respect to composite (wt.%), load (N) and speed (rpm)

In this investigation, the variation in the wear rate was calculated with respect to the reinforcement (wt.%), load (N) and speed (rpm). Figure 10 depicts the variation in the wear rate ($\mu\text{m/s}$) with respect to the amount of reinforcement (wt.%) as a function of speed (rpm). It was clearly evident from the figure that wear occurred in all the composites with the various wt.% of the reinforcement. The wear rate ($\mu\text{m/s}$) decrease with increase in reinforcement (wt.%) at various speeds from 100 rpm to 700 rpm respectively. It is observed that the wear loss is greater in the matrix material and less in the composite with 6 wt.% of reinforcement. The presence of reinforcing particles with silicon content as well as good interfacial bonding between the matrix and reinforcement phase increased the hardness, and hence enhanced the strength of the composite. Figure 11 depicts the variation in the wear rate ($\mu\text{m/s}$) with respect to speed (rpm), varying from 100 rpm to 700 rpm as a function of reinforcement varying from 0% to 6 wt.%.

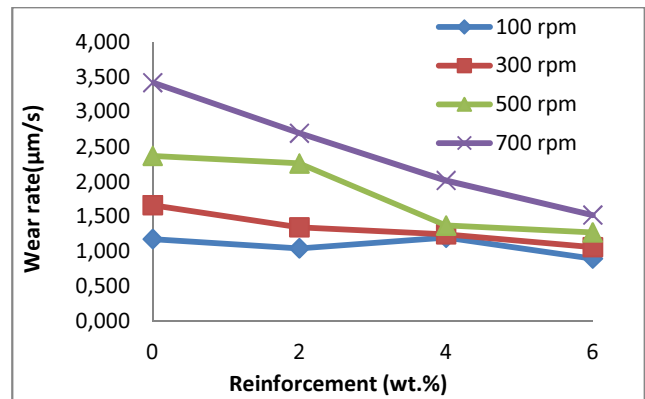


Fig. 10. Variation in wear rate ($\mu\text{m/s}$) with amount of reinforcement [wt.%]

Figure 11 reveals that the wear rate ($\mu\text{m/s}$) of the matrix material and composites rose with the increase in speed (rpm), ranging from 100 rpm to 700 rpm. The maximum wear rate ($\mu\text{m/s}$) was observed for the matrix material at 700 rpm with the minimum wear rate ($\mu\text{m/s}$) for the composite with 6 wt.% reinforcement at 100 rpm. The wear rate ($\mu\text{m/s}$) of the composites went up with the increase in speed because of the unavoid-

able rise in the temperature of the material as the speed increased, which caused a reduction in the wear resistance of the material.

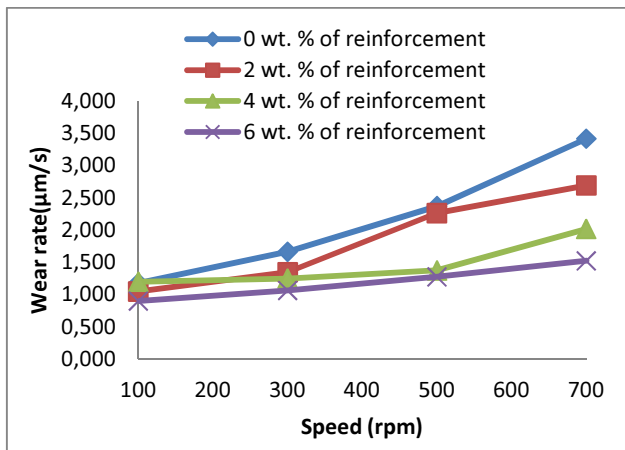


Fig. 11. Variation in wear rate [$\mu\text{m/s}$] with speed (rpm)

The variation in the wear rate ($\mu\text{m/s}$) with respect to load (N) varying from 10 to 40 N as a function of reinforcement varying from 0 to 6 wt.% is shown in Figure 12. The wear rate ($\mu\text{m/s}$) of the composites grew with the increase in load from 10 to 40 N with the maximum wear rate ($\mu\text{m/s}$) for the matrix material at all the loads (N) when compared with the composites.

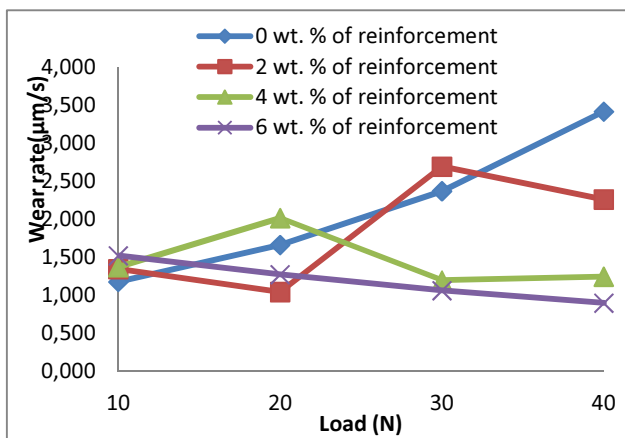


Fig. 12. Variation in wear rate ($\mu\text{m/s}$) with load (N)

Figure 12 shows large variation in the peaks with the increase in reinforcement wt.% is because of the experimental layout obtained from the L_{16} orthogonal array, as the experiment was performed to obtain the minimum wear rate ($\mu\text{m/s}$) by varying all the possible input parameters. The enhancement in wear resistance of the composite is attributed to the increase in the hardness of the composite [21, 22] because of the presence of silicon microballoons.

Variation in coefficient of friction with respect to reinforcement (wt.%), load (N) and speed (rpm)

The effect on the coefficient of friction is studied as a function of wt.% of the reinforcement, load (N) and speed (rpm) and is shown in Figures 13-15. These

curves illustrate that the coefficients of friction for the composites are lower than that of the matrix material. The pattern of curves from the graphs was because of the presence of reinforcing particles, which took the load at the interface between the contacting surfaces during sliding. The influence of the increase in the wt.% of reinforcement lowered the coefficient of friction, but the coefficient of friction rose with respect to speed from 100 to 700 rpm with respect to the wt.% of the reinforcement. The minimum value of the coefficient of friction was found at the lower speed and at low loads, with a gradually rising trend with respect to the increase in speed and load.

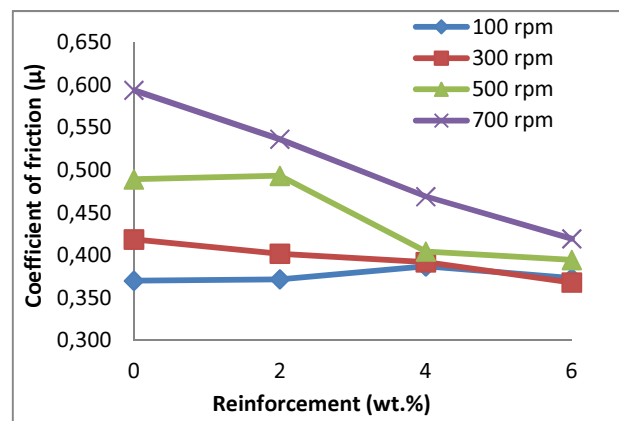


Fig. 13. Variation in coefficient of friction (μ) with amount of reinforcement [wt.%]

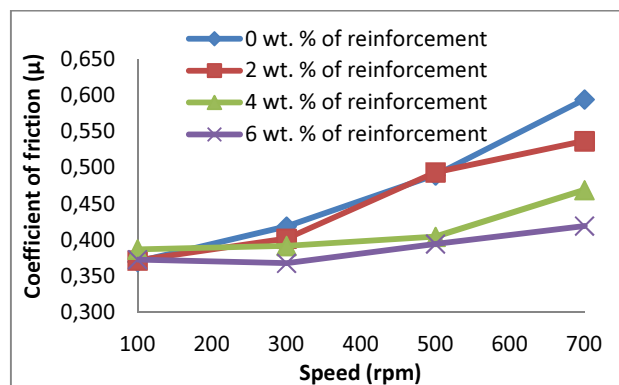


Fig. 14. Variation in coefficient of friction (μ) with speed (rpm)

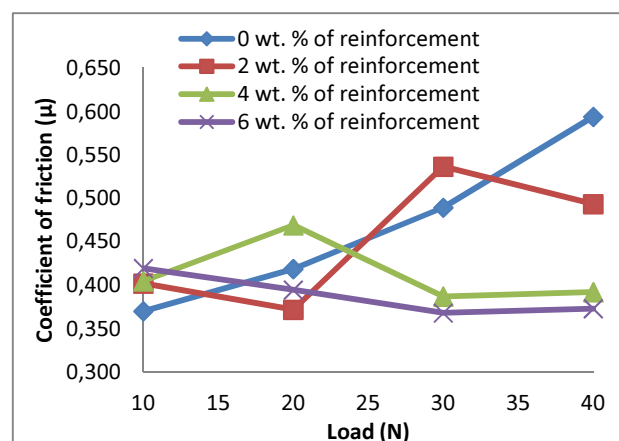


Fig. 15. Variation in coefficient of friction (μ) with load (N)

Optimization technique

In this study, the analysis is carried out by reinforcing the matrix material with various wt.% (0, 2, 4, 6) of reinforcement. The Taguchi L_{16} orthogonal array with three factors at four levels for the input is considered as shown in Table 9. The considered input parameters and the obtained output parameters as per the L_{16} orthogonal array are shown in Table 10. The Taguchi method was used for analysis of the data to obtain the optimal combination of input parameters [23]. The Taguchi analysis was performed individually on both of the output parameters, i.e. on the wear rate ($\mu\text{m/s}$) and the coefficient of friction for obtaining their optimal values. The experiment was performed on 16 specimens in a set of four for each of the wt.% (0, 2, 4, 6) of the reinforcement. From the experiment, the values for the wear rate and coefficient of friction were obtained for all the 16 specimens. The minimum value of the wear rate is $0.901 \mu\text{m/s}$, obtained for the composite with 6 wt.% of reinforcement at 100 rpm and 40 N.

The obtained minimum value of the coefficient of friction is 0.368 for the composite with 6 wt.% of reinforcement at 300 rpm and 30 N. The means and S/N are calculated for both the responses individually.

TABLE 9. Control factors and their levels

Control factors	Levels			
	1	2	3	4
Reinforcement	0	2	4	6
Speed	100	300	500	700
Load	10	20	30	40

TABLE 10. Input parameters and output parameters of matrix material and composites

Experiment number	Input parameters			Output parameters	
	Reinforcement [wt.%]	Speed [rpm]	Load [N]	Wear rate [$\mu\text{m/s}$]	Coefficient of friction
1	0	100	10	1.180	0.370
2	0	300	20	1.666	0.419
3	0	500	30	2.373	0.489
4	0	700	40	3.420	0.594
5	2	100	20	1.048	0.372
6	2	300	10	1.349	0.402
7	2	500	40	2.264	0.493
8	2	700	30	2.695	0.537
9	4	100	30	1.200	0.387
10	4	300	40	1.250	0.392
11	4	500	10	1.375	0.405
12	4	700	20	2.020	0.469
13	6	100	40	0.901	0.373
14	6	300	30	1.065	0.368
15	6	500	20	1.276	0.395
16	6	700	10	1.524	0.419

Signal-to-noise ratio (S/N)

The wear rate is one of the influencing factors to obtain better quality of the composite, which is also dependent on the coefficient of friction between the contacting surfaces. The effect of the input parameters on the output responses can be investigated by finding the means and signal-to-noise ratios for each of the considered factors. In this analysis, the smaller the better condition is considered for both the wear rate and coefficient of friction to obtain better responses. Statistical analysis software, Minitab was utilized to ascertain the influence of the input parameters on the responses. Tables 11 and 12 give the response values of means for wear rate and coefficient of friction. Tables 13 and 14 show the response values of S/N for the wear rate and coefficient of friction.

TABLE 11. Response values of means for wear rate

Level	Reinforcement [wt.%]	Speed [rpm]	Load [N]
1	2.16	1.082	1.357
2	1.839	1.333	1.502
3	1.461	1.822	1.833
4	1.192	2.415	1.959
Delta	0.968	1.332	0.602
Rank	2	1	3

For better bonding of the reinforcing particles in to the matrix material, a smaller value of S/N is considered. The main effect plots for the means and S/N are obtained from the statistical analysis software, Minitab and are in shown in Figures 16-19 for the wear rate and coefficient of friction.

TABLE 12. Response values of means for coefficient of friction

Level	Reinforcement [wt.%]	Speed [rpm]	Load [N]
1	0.468	0.3755	0.3989
2	0.4509	0.3951	0.4135
3	0.4131	0.4455	0.4452
4	0.3887	0.5047	0.4631
Delta	0.0792	0.1293	0.0642
Rank	2	1	3

TABLE 13. Response values of S/N for wear rate

Level	Reinforcement [wt.%]	Speed [rpm]	Load [N]
1	-6.0144	-0.6307	-2.6159
2	-4.679	-2.3797	-3.2662
3	-3.0987	-4.8716	-4.5619
4	-1.3546	-7.2646	-4.7027
Delta	4.6599	6.6339	2.0868
Rank	2	1	3

TABLE 14. Response values of S/N for coefficient of friction

Level	Reinforcement [wt.%]	Speed [rpm]	Load [N]
1	6.733	8.51	7.991
2	7.014	8.075	7.703
3	7.705	7.071	7.136
4	8.218	6.014	6.84
Delta	1.485	2.496	1.151
Rank	2	1	3

From the values obtained from the means as shown in Table 11, the most propitious parameters to obtain the minimum wear rate are the composite with 6 wt.% of reinforcement, speed of 100 rpm and load of 10 N. The trend of the curve in Figure 16 indicates that the wear rate was mostly influenced by the variation in speed, followed by reinforcement (wt.%) and load (N). From the values obtained from S/N as shown in Figure 18, it is evident that the wear rate is highly dependent on the speed and a better wear rate was obtained at minimum speed. The increasing trend of S/N for the reinforcement (wt.%) proves that the wear rate decreased with the increase in reinforcement (wt.%). The curve for the load shows that a better output was obtained at the load of 10 N. The slope of the curve for the load shows a decreasing trend from 10 to 40 N with a variation in the slope at each of the levels of load.

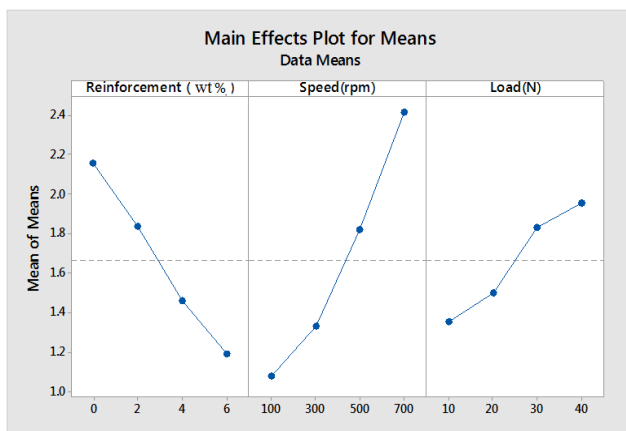


Fig. 16. Main effects plot for means of wear rate

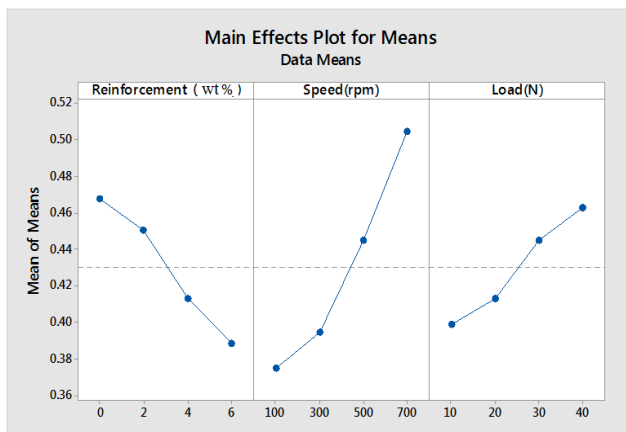


Fig. 17. Main effects plot for means of coefficient of friction

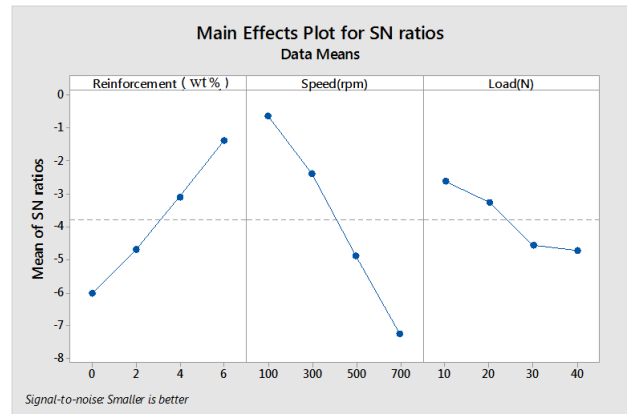


Fig. 18. Main effects plot for S/N of wear rate

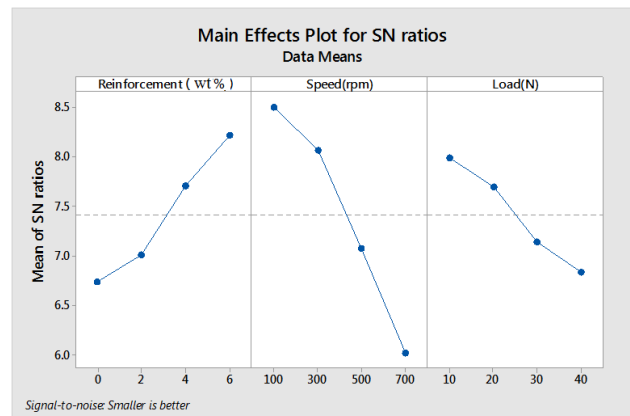


Fig. 19. Main effects plot for S/N of coefficient of friction

From the values obtained from the means as shown in Table 12, the optimal parameters for the obtained minimum coefficient of friction are reinforcement 6 wt.%, speed of 100 rpm and load of 10 N. The trend of the curve in Figure 17 illustrates that the coefficient of friction was mostly influenced by the variation in speed followed by reinforcement (wt.%) and load (N). From the values obtained from S/N as shown in Figure 19, it is evident that the coefficient of friction was mostly influenced by the variation in speed followed by reinforcement (wt.%) and load (N). The enhancement of wear resistance is mainly because of the addition of reinforcement to the matrix material, which increased the strength of the composite as the contribution of reinforcement increased. The response tables of the wear rate and coefficient of friction reveal that 6 wt.% reinforcement, speed of 100 rpm and load of 10 N are the optimal parameters, respectively.

Analysis of variance (ANOVA)

ANOVA was conducted to investigate the influence of the process parameters in obtaining the minimum wear rate and coefficient of friction [24]. The contribution of individual process parameters and the influence of the process parameters on one another can also be studied from the results of ANOVA. The statistical analysis software Minitab was used in this study to perform analysis of variance for obtaining the minimum wear rate and coefficient of friction.

TABLE 15. ANOVA results for wear rate

Source	DF	Seq.SS	Adj.SS	Adj.MS	F-Value	P-Value	Contribution [%]
Reinforcement [wt. %]	3	2.163	2.163	0.721	24.56	0.001	29.11
Speed [rpm]	3	4.1476	4.1476	1.38255	47.1	0.000	55.82
Load [N]	3	0.9434	0.9434	0.31447	10.71	0.008	12.70
Error	6	0.1761	0.1761	0.02935			2.37
Total	15	7.4302					100.00

TABLE 16. ANOVA results for coefficient of friction

Source	DF	Seq.SS	Adj.SS	Adj.MS	F-Value	P-Value	Contribution [%]
Reinforcement [wt. %]	3	0.01546	0.01546	0.005153	16.86	0.003	22.87
Speed [rpm]	3	0.04006	0.04006	0.013352	43.68	0.000	59.25
Load [N]	3	0.01025	0.01025	0.003417	11.18	0.007	15.16
Error	6	0.00183	0.00183	0.000306			2.71
Total	15	0.0676					100.00

Seq.SS - sequential sum of squares; adj.SS - adjusted sum of squares; Adj.MS - adjusted mean of squares; F - statistical Test; P - statistical value

TABLE 17. Normalization, deviation sequence, grey relational coefficient and rank

Experiment No.	Wear rate [$\mu\text{m/s}$]	COF	Normalization		Deviation sequence		Grey relational coefficient		GRG	RANK
			Wear rate [$\mu\text{m/s}$]	COF	Wear rate [$\mu\text{m/s}$]	COF	Wear rate [$\mu\text{m/s}$]	COF		
1	1.180	0.370	0.889	0.991	0.111	0.009	0.819	0.983	0.901	4
2	1.666	0.419	0.696	0.776	0.304	0.224	0.622	0.691	0.656	11
3	2.373	0.489	0.416	0.463	0.584	0.537	0.461	0.482	0.472	14
4	3.420	0.594	0.000	0.000	1.000	1.000	0.333	0.333	0.333	16
5	1.048	0.372	0.942	0.983	0.058	0.017	0.895	0.967	0.931	3
6	1.349	0.402	0.822	0.850	0.178	0.150	0.738	0.769	0.753	8
7	2.264	0.493	0.459	0.445	0.541	0.555	0.480	0.474	0.477	13
8	2.695	0.537	0.288	0.254	0.712	0.746	0.412	0.401	0.407	15
9	1.200	0.387	0.881	0.916	0.119	0.084	0.808	0.856	0.832	5
10	1.250	0.392	0.861	0.894	0.139	0.106	0.783	0.825	0.804	6
11	1.375	0.405	0.812	0.838	0.188	0.162	0.727	0.756	0.741	9
12	2.020	0.469	0.556	0.553	0.444	0.447	0.530	0.528	0.529	12
13	0.901	0.373	1.000	0.978	0.000	0.022	1.000	0.958	0.979	1
14	1.065	0.368	0.935	1.000	0.065	0.000	0.885	1.000	0.942	2
15	1.276	0.395	0.851	0.882	0.149	0.118	0.771	0.809	0.790	7
16	1.524	0.419	0.753	0.773	0.247	0.227	0.669	0.687	0.678	10

The results of ANOVA are presented in Table 15 for the wear rate and in Table 16 for the coefficient of friction.

The results of ANOVA for the wear rate and coefficient of friction reveal that speed (rpm) is the prominent process factor with a major contribution, followed by reinforcement (wt.%) and load (N).

From Table 15, for the wear rate, speed (rpm) contributes 55.82%, followed by reinforcement (wt. %) 29.11% and load (N) 12.70%. From Table 16, for the

coefficient of friction, speed (rpm) contributes 59.25%, followed by reinforcement (wt.%) 22.87% and load (N) 15.16%.

For a confidence level of 95%, the p-value for all the factors for the wear rate and coefficient of friction were less than 0.05, indicating that all the factors have a significant influence on the responses.

In the present study, optimal process parameters are obtained individually for the minimum wear rate and minimum coefficient of friction. Notwithstanding, in

reality the optimal process parameters for the minimum wear rate and coefficient of friction are essential. Hence, in this study, Grey Relational Analysis (GRA) was performed to obtain a unique set of optimal parameters for both the responses.

GRA for multi response optimization

GRA is employed in cases with a limited set of experimental data. It is generally applied in systems to analyze and optimize the process parameters with multiple responses [25-28]. Pre-processing of the experimental data i.e., responses was done to generate Grey Relational Grades (GRGs). The standard procedure for grey relational analysis was followed and the values of normalizing, deviation sequences, grey relational coefficient for the wear rate and coefficient of friction along with grey relational grade and corresponding rank are shown in Table 17.

Statistical analysis software Minitab was used to generate the values of the means and S/N considering the larger the better method for S/N, as the objective is to maximize GRG.

CONCLUSIONS

- In the present investigation, various wt. % (2, 4, 6) of silicon hollow glass microsphere reinforcement was added to Al 4032 matrix material, mixed well and stir cast to fabricate composites of required shapes and sizes as per ASTM standards for conducting experiments to determine various mechanical properties.
- EDX analysis was carried out on the composites, which shows the presence of reinforcement in the matrix material.
- The physical properties such as the density and porosity of the composites with variable wt. % (0, 2, 4, 6) of reinforcement are found and the results show that the density of the composites drops with the increase in wt.% of the reinforcement, and the porosity (%) rises with the increase in wt.% of the reinforcement.
- SEM investigations performed on the specimens reveals that nearly uniform distribution of the reinforcement in the matrix material was achieved because of the stir casting method. The presence of reinforcement led to refinement of the grain structure and the values of the average grain size measured using ImageJ are 42.06, 30.88, 23.72 and 15.21 μm , respectively for the composites with 0, 2, 4, 6 wt.% of reinforcement.
- The experiments to determine the mechanical properties such as hardness, tensile strength and compressive strength were conducted as per ASTM standards on specimens with reinforcement of 0, 2, 4, 6 wt.%. The results revealed that the values of the mechanical properties increased with the addition of reinforcement to the matrix material.
- Furthermore, the mechanical properties showed growth in their value with the increase in wt.% of the reinforcement. The addition of reinforcement attributed to the increase in these properties.
- The tribological behavior of the composites was studied by performing wear tests on a pin-on-disc apparatus and the variation in the wear rate and coefficient of friction of the composites with reinforcement of 0, 2, 4, 6 wt.% were studied with respect to the reinforcement (wt.%), speed (rpm) and load (N). The results reveal that the values of the wear rate and coefficient of friction were reduced by the addition of reinforcement when compared to the matrix material. What is more, the wear resistance of the composites rose with the increase in wt. % of the reinforcement.
- The micro-structural analyses of the worn surfaces reveal the formation of cracks with the increase in load. In addition, the effect of erosion is predominant because of de-lamination at higher speeds.
- The Taguchi L_{16} orthogonal array was used independently to ascertain the influential process parameters for obtaining the minimum wear rate and minimum coefficient of friction, which were found to be the composite with 6 wt.% of reinforcement at the speed of 100 rpm and load of 40 N as well as 6 wt.% of reinforcement at the speed of 300 rpm and load of 30 N.
- Multi-response optimization was performed using grey relational analysis to ascertain the influential process parameters considering both the minimum wear rate and minimum coefficient of friction, which were found in the composite with 6 wt.% of reinforcement at the speed of 100 rpm and load of 40 N.
- The response tables for the means and S/N reveals that 6 wt.% reinforcement at the speed of 100 rpm and load of 10 N were the optimal parameters for the minimum wear rate and minimum coefficient of friction from both the Taguchi and grey relational analyses.
- ANOVA was performed to determine the percentage contribution of individual process parameters on the wear rate and coefficient of friction. It was observed that speed is the most contributing factor with 55.82% followed by reinforcement (wt. %) 29.11% and load with 12.70% on the wear rate. Moreover, the effect of the parameters followed the same trend on the coefficient of friction also with speed as the most influential parameter contributing 59.25% followed by reinforcement (wt.%) 22.87% and load with 15.16%.

REFERENCES

- [1] Hiroake N., Kenjie K., Akinori N., Development of aluminum metal matrix composites (Al-MMC) brake rotor and pad, *JSAE Rev.* 2002, 23, 3, 365-370.

- [2] Gudimetla A., Sambhu Prasad S., Lingaraju D., Tribological studies of aluminium metal matrix composites with micro reinforcements of silicon and silicon balloons, *Mater. Today Proc.* 2019, 18, 47-56.
- [3] Chen Z., Wang T., Zheng Y., Zhao Y., Kang H., Gao L., Development of TiB₂ reinforced aluminum foundry alloy based in situ composites – Part I: An improved halide salt route to fabricate Al-5wt%TiB₂ master composite, *Mater. Sci. Eng. A* 2014, 605, 301-309.
- [4] Schmidt H., Hattel J., Modelling heat flow around tool probe in friction stir welding, *Sci. Technol. Weld. Join.* 2005, 10, 2, 176-186.
- [5] Matters Q., *Quality Matters Newsletter* 2003, II.
- [6] Balaji G.K., Muthukumaran S., Senthilkumaran S., Pradeep A., Optimization of friction welding of tube-to-tube plate using an external tool with filler plate, *J. Mater. Eng. Perform.* 2012, 21, 7, 1199-1204.
- [7] Rengasamy N.V., Rajkumar M., Senthil Kumaran S., Mining environment applications on Al 4032 - ZrB₂ and TiB₂ in-situ composites, *J. Alloys Compd.* 2016, 658, 757-773.
- [8] Çiçek A., Kıvık T., Ekici E., Optimization of drilling parameters using Taguchi technique and response surface methodology (RSM) in drilling of AlSi 304 steel with cryogenically treated HSS drills, *J. Intell. Manuf.* 2015, 26, 2, 295-305.
- [9] Lingaraju D., Ramji K., Mohan Rao N.B.R., Rajya Lakshmi U., Characterization and prediction of some engineering properties of polymer – Clay/silica hybrid nanocomposites through ANN and regression models, *Procedia Eng.* 2011, 10, 9-18.
- [10] Natarajan S., Narayanasamy R., Kumaresh Babu S.P., Dinesh G., Anil Kumar B., Sivaprasad K., Sliding wear behaviour of Al 6063/TiB₂ in situ composites at elevated temperatures, *Mater. Des.* 2009, 30, 7, 2521-2531.
- [11] Xiuqing Z., Haowei W., Lihua L., Xinying T., Naiheng M., The mechanical properties of magnesium matrix composites reinforced with (TiB₂ + TiC) ceramic particulates, *Mater. Lett.* 2005, 59, 17, 2105-2109.
- [12] Pathak J.P., Singh J.K., Mohan S., Synthesis and characterisation of aluminium-silicon-silicon carbide composite, *Indian J. Eng. Mater. Sci.*, 2006, 13, 3, 238-246.
- [13] Lü L., Lai M.O., Su Y., Teo H.L., Feng C.F., In situ TiB₂ reinforced Al alloy composites, *Scr. Mater.* 2001, 45, 9, 1017-1023.
- [14] Han Y., Liu X., Bian X., In situ TiB₂ particulate reinforced near eutectic Al-Si alloy composites, *Compos. – Part A Appl. Sci. Manuf.* 2002, 33, 3, 439-444.
- [15] Wu S., Zone-melted unidirectional solidification of 2001, 6, 225-229.
- [16] Michael Rajan H.B., Ramabalan S., Dinaharan I., Vijay S.J., Synthesis and characterization of in situ formed titanium diboride particulate reinforced AA7075 aluminum alloy cast composites, *Mater. Des.* 2013, 44, 438-445.
- [17] Hassan A.M., Alrashdan A., Hayajneh M.T., Mayyas A.T., Wear behavior of Al-Mg-Cu-based composites containing SiC particles, *Tribol. Int.* 2009, 42, 8, 1230-1238.
- [18] Savaşkan T., Bican O., Dry sliding friction and wear properties of Al-25Zn-3Cu-(0-5)Si alloys in the as-cast and heat-treated conditions, *Tribol. Lett.* 2010, 40, 3, 327-336.
- [19] Lee J.M., Kang S.B., Han J., Dry sliding wear of MAO-coated A356/20 vol.% SiCp composites in the temperature range 25-180°C, *Wear* 2008, 264, 1-2, 75-85.
- [20] Rao R.N., Das S., Mondal D.P., Dixit G., Dry sliding wear behaviour of cast high strength aluminium alloy (Al-Zn-Mg) and hard particle composites, *Wear* 2009, 267, 9-10, 1688-1695.
- [21] Ramesh C.S., Keshavamurthy R., Channabasappa B.H., Ahmed A., Microstructure and mechanical properties of Ni-P coated Si₃N₄ reinforced Al6061 composites, *Mater. Sci. Eng. A* 2009, 502, 1-2, 99-106.
- [22] Mandal A., Chakraborty M., Murty B.S., Ageing behaviour of A356 alloy reinforced with in-situ formed TiB₂ particles, *Mater. Sci. Eng. A* 2008, 489, 1-2, 220-226.
- [23] Senthil Kumaran S., Muthukumaran S., Vinodh S., Optimization of friction welding of tube-to-tube plate using an external tool by Taguchi method and genetic algorithm, *Int. J. Adv. Manuf. Technol.* 2011, 57, 1-4, 167-182.
- [24] Express M., Example of One-Way ANOVA 2020, 4-6.
- [25] Zhang D., Chen M., Wu S., Liu J., Amirghani S., Analysis of the relationships between waste cooking oil qualities and rejuvenated asphalt properties, *Materials (Basel)* 2017, 10, 5.
- [26] Zou S.Y., Huang R., Chi M.C., Hsu H.M., Factors affecting the effectiveness of inorganic silicate sealer material through multi-quality characteristics, *Materials (Basel)* 2013, 6, 3, 1191-1204.
- [27] Wojciechowski S., Maruda R.W., Krolczyk G.M., Niesłony P., Application of signal to noise ratio and grey relational analysis to minimize forces and vibrations during precise ball end milling, *Precis. Eng.* 2018, 51, 582-596.
- [28] Kasemsiri P., Dulsang N., Pongsa U., Hiziroglu S., Chindaprasirt P., Optimization of biodegradable foam composites from cassava starch, oil palm fiber, chitosan and palm oil using Taguchi method and grey relational analysis, *J. Polym. Environ.* 2017, 25, 2, 378-390.